f → d transition energies of divalent lanthanides in inorganic compounds

2003 J. Phys.: Condens. Matter 15 575

(http://iopscience.iop.org/0953-8984/15/3/322)

INSTITUTE OF PHYSICS PUBLISHING JOURNAL OF PHYSICS: CONDENSED MATTER

J. Phys.: Condens. Matter **15** (2003) 575–594 PII: S0953-8984(03)55450-9

f → d transition energies of divalent lanthanides in inorganic compounds

P Dorenbos

Interfaculty Reactor Institute, Delft University of Technology, Mekelweg 15, 2629 JB Delft, The Netherlands

E-mail: dorenbos@iri.tudelft.nl

Received 1 November 2002
Published 13 January 2003
Online at stacks.iop.org/JPhysCM/15/575

Abstract

The systematic in the $4f^n \rightarrow 4f^{n-1}5d$ transition energy of divalent lanthanides in inorganic compounds has been studied. Energies were derived from excitation and optical absorption spectra gathered from the literature. Going through the lanthanide series from La^{2+} to Yb^{2+}, a characteristic variation is observed similar to that known for the trivalent lanthanides and the free atoms and free ions. Once the transition energy is known for one lanthanide in a compound, that of all others in that same compound can be predicted. The value for the Stokes shift between fd excitation and df emission appears independent of the lanthanide ion. For Gd^{2+} to Yb^{2+} both the spin-forbidden and the spin-allowed fd-transition energies are discussed.

1. Introduction

Lanthanides with electron configuration $[Xe]4f^n6s^m$ form an important class of activator ions in inorganic compounds for many luminescence applications. As atoms or as free ions the 6s shell can be empty, occupied by one electron ($m = 1$) or occupied by two electrons ($m = 2$). In compounds, the 6s shell is empty, and in going through the lanthanide series from La to Lu, the 4f shell is filled with at most $n = 14$ electrons. They are effectively shielded from the environment by the filled $5p^6$ and $5s^2$ shells of the [Xe] configuration. As a result, the energies of the numerous $4f^n$ levels are not much influenced by the crystalline environment. The shielding of an electron in a 5d orbital, on the other hand, is relatively poor and its energy is very sensitive to the environment.

Generally, the energy $E(n, m, Q, \mathrm{A})$ needed to excite an electron from the ground state of the $4f^n6s^m$ configuration to the lowest energy of the $4f^{n-1}6s^m$ 5d configuration depends on the type of lanthanide ion (characterized by n, m and its ionic charge Q) and the host crystal denoted by A. Figure 1 shows $E(n, m, Q, \mathrm{free})$ for the lanthanides in free space (A = free) as a function of n. This figure is similar to that presented by Brewer [2] and Martin [3] but updated with new experimental data acquired later [4, 5]. In figure 1 and throughout the rest

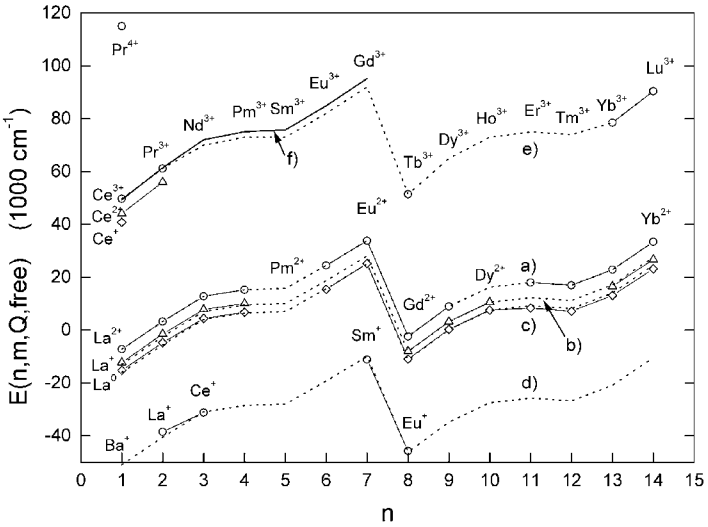

Figure 1. fd transition energies $E(n, m, Q, \text{free})$ for the free atomic and ionic lanthanides. O, $m = 0$; △, $m = 1$; ◇, $m = 2$. Curve (a): $E(n, 0, 2+, \text{free})$ with estimated values for Pm^{2+} and Dy^{2+}. A downward shift of curve (a) by −5750, −8800 and −43 770 cm^{-1} yields curves (b), (c) and (d), respectively. Curve (e): predicted $E(n, 0, 3+, \text{free})$ curve by Brewer [5]. Curve (f): $E_{\text{A free}}(n \leqslant 7, 3+)$ from [11].

of this work it was chosen to express the energy in terms of the wavenumber in cm^{-1}. It is the reciprocal of the wavelength and 1 eV corresponds to 8065 cm^{-1}.

Data are most complete for the neutral atoms with $m = 2$ (curve (c)) and the divalent lanthanides with $m = 0$ (curve (a)). The differential (dE/dn) as a function of n for both series is practically identical. The same applies for the available data for the monovalent lanthanides with $m = 1$ (curve (b)) and $m = 0$ (curve (d)). The energy is large when the 4f shell is filled ($n = 14$) or half-filled ($n = 7$), and it is small for $n = 1$ and 8. This characteristic pattern is well understood. It has been described by Jörgensen's refined electron-spin-pairing-energy theory [6–8] and can be reproduced very well from first principle calculations [9].

For most of the trivalent lanthanides with $m = 0$, experimental data on the fd-transition energy are not known. Based on the fourth ionization potentials and by comparison with the divalent lanthanides Brewer [2] and later Sugar and Reader [10] predicted the values for the missing data on $E(n, 0, 3+, \text{free})$. Curve (e) through the data on the trivalent lanthanides in figure 1 is from the prediction by Brewer [5].

In a recent study on $E(n, 0, 3+, \text{A})$ for all 13 trivalent lanthanides in about 300 different inorganic compounds [11, 12], it was found that the following simple expression applies:

$$E(n, 3+, \text{A}) = 49\,340 + \Delta E(n, 1, 3+) - D(3+, \text{A}) \equiv E_{\text{A free}}(n, 3+) - D(3+, \text{A}) \quad (1)$$

where

$$\Delta E(n, 1, 3+) \equiv \overline{E(n, 3+, \text{A}) - E(1, 3+, \text{A})}. \quad (2)$$

The parameter m has been omitted in $E(n, 3+, \text{A})$ since, in compounds, lanthanide ions have an empty 6s shell. $n = 1$ pertains to Ce^{3+} and $n = 14$ to Lu^{3+}. 49 340 cm^{-1} (6.12 eV) is the energy $E(1, 0, 3+, \text{free})$ of the free Ce^{3+} ion. The difference between the fd-transition energy for the lanthanide with $4f^n$ electrons with that of Ce^{3+} was found to be independent of the type of compound. The values averaged over all compounds are denoted by $\Delta E(n, 1, 3+)$ and can be found in [11]. The redshift $D(3+, \text{A})$ represents the lowering of the fd-transition energy

when the lanthanide ion is brought from the gaseous state into compound A. Once this value is known for, say, Ce^{3+}, equation (1) predicts the fd-transition energies of all other lanthanides.

The data on $E(n, m, Q, \text{free})$ and the data on $E(n, 3+, \text{A})$ demonstrate that $\mathrm{d}E/\mathrm{d}n$ does not depend much on Q, m and A. Apparently, the 'internal' environment of the lanthanide ion, i.e. the ionic charge and the filling state of the 6s shell, does not affect $\mathrm{d}E/\mathrm{d}n$ despite that E itself may change by 100 000 cm^{-1} (12.4 eV), see figure 1. Also the influence of the environment 'external' to the trivalent lanthanide, i.e. the host crystal, is very small despite the fact that the redshift $D(3+, \text{A})$ may amount to 30 000 cm^{-1} (3.72 eV) [12]. It is now expected that $\mathrm{d}E/\mathrm{d}n$ will also be the same for the divalent lanthanides in compounds, and then the following relationship should apply:

$$E(n, 2+, \text{A}) = E(7, 0, 2+, \text{free}) + \Delta E(n, 7, 2+) - D(2+, \text{A}) \equiv E_{\text{A free}}(n, 2+) - D(2+, \text{A}), \tag{3}$$

where now $n = 1$ pertains to La^{2+} and $n = 14$ to Yb^{2+}. Since most data are available on Eu^{2+} in compounds, Eu^{2+} with $n = 7$ has been chosen as our lanthanide of reference. $\Delta E(n, 7, 2+)$ and $E_{\text{A free}}(n, 2+)$ are defined similar to those for the trivalent lanthanides.

The present work is part of a study with several objectives.

(1) Collecting information on $E(n, 2+, \text{A})$ by analysing spectroscopic data gathered from the literature.
(2) Establishing to what extent equation (3) applies for the divalent lanthanides in compounds and establishing the values for $\Delta E(n, 7, 2+)$ and $E_{\text{A free}}(n, 2+)$.
(3) Compiling values for the redshift $D(2+, \text{A})$ in inorganic compounds.
(4) Analysing the relationship between $D(2+, \text{A})$ and the crystalline environment.

This paper is concerned with objectives 1 and 2. First, the main features of the spectroscopic properties of the divalent lanthanides in compounds are discussed. This is required for a correct interpretation of excitation and absorption spectra, and to obtain reliable and consistent values for $E(n, 2+, \text{A})$. Next, data on $E(n, 2+, \text{A})$ are presented. For $n > 7$, $E(n, 2+, \text{A})$ values are provided for the first spin-allowed fd and spin-forbidden fd transitions. In the case of Eu^{2+}, Sm^{2+}, Tm^{2+} and Yb^{2+} information on df luminescence is provided. The general validity of equation (3) will be demonstrated, and finally its predictive potential is commented on. The results of this work, combined with the third and fourth objectives (to be dealt with in [32]), provide a database enabling us to predict $E(n, 2+, \text{A})$ of yet uninvestigated combinations of divalent lanthanides and compounds.

The analysis in this work will be purely empirical. The physics behind equation (3) and the relationship between redshift $D(2+, \text{A})$ and the type of crystalline environment is not addressed. These aspects are expected to be very similar to those for the trivalent lanthanides treated in [13–15] and in references therein.

2. General properties of the divalent lanthanides

General features of fd-excitation and absorption spectra of the divalent lanthanides in alkaline earth fluorides can be found in the early works by McClure and Kiss [16] and Loh [17]. An extensive review of the divalent lanthanides in halide compounds was presented later by Rubio [18]. Below, several aspects will be discussed that are needed for interpretation of the spectra.

Since the most intense fd bands in spectra are those belonging to transitions that are spin-allowed, it is of relevance to know the total electron spin of the initial and final states. Figure 2 shows the energy level diagram belonging to the $4f^n$ configuration of the free divalent

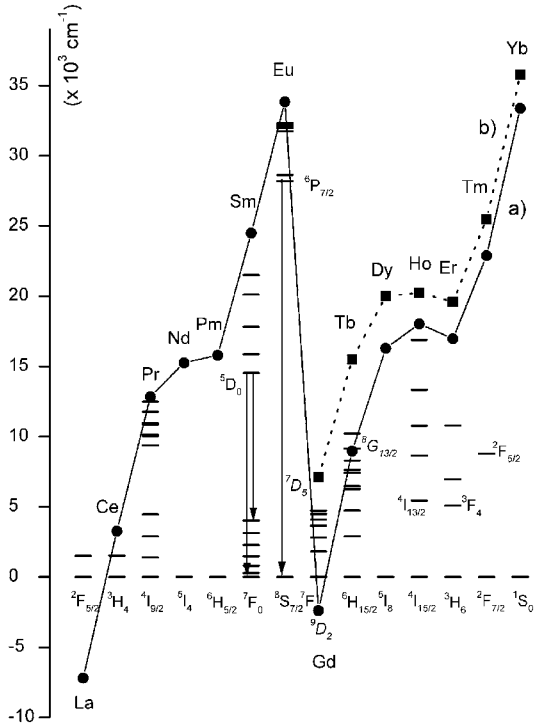

Figure 2. $4f^n$ energy level scheme of the free divalent lanthanides from [4]. The full curve (a) connects the first fd level. This is $E^{sa}_{\text{A free}}(n, 2+)$ for $n \leqslant 7$ and $E^{sf}_{\text{A free}}(n, 2+)$ for $n > 7$. The broken curve (b) represents $E^{sa}_{\text{A free}}(n, 2+)$ for $n > 7$.

lanthanides. The data were obtained from the tabulations in [4]. The levels were not specified for Nd, Pm and Dy.

The spin multiplicity of the lowest $4f^n[^{2S+1}L_J]$ level increases from $2S + 1 = 2$ for La^{2+} up to 8 for Eu^{2+}, and then decreases to 1 for the $4f^{14}[^1S_0]$ level in Yb^{2+}. In the excited $4f^{n-1}5d$ configuration, the exchange interaction tends to align the spin of the 5d electron with the total spin vector of the $n-1$ electrons that have remained in the 4f shell. Applying pure LS coupling together with Hund's rule we find that the highest spin (HS) LS-term has the lowest energy. However, the levels are not pure and low spin (LS) states are admixed with the HS state. For Ce^{2+}, where the exchange interaction between the 5d electron and the 4f electron is small, the lowest fd state is 72% LS $^1G_4$ character with 22% HS $^3H_4$ mixed in [4]. Proceeding to Eu^{2+}, where the exchange interaction with the six electrons in the 4f shell is much stronger, the first fd state is almost entirely of HS character, i.e. 97% ^8H with only 2% ^6G [4]. Since the lowest energy fd state for $n \leqslant 7$ always has HS character with the same spin multiplicity as the $4f^n$ ground state, transitions between them are always spin- and dipole-allowed.

The situation is different for $n > 7$, where the lowest $4f^{n-1}5d$ level has higher spin than the ground state $4f^n$ level and transitions between them are spin-forbidden. As in Eu^{2+}, the exchange interaction is large in Gd^{2+}. The lowest fd state is almost pure HS $^9D_2$ with only 1% LS ^7D admixed [4]. The first LS state is a level with 97% $^7D_5$ and 3% ^9D found 9356 cm^{-1} above the $^9D_2$ level [4]. For the heavy lanthanides Tm^{2+} and Yb^{2+}, the total spin of the $4f^{n-1}$ part of the electron configuration is again small and exchange interaction is expected to be small also. Experimentally this has been observed already for the trivalent lanthanides [11, 19]. In

order to discriminate between spin-forbidden and spin-allowed transition energies for $n > 7$, we will denote them as E^{sf} and E^{sa}, respectively. Figure 2 shows the values for $E^{sa}_{\text{A free}}(n, 2+)$ and $E^{sf}_{\text{A free}}(n, 2+)$, as will be determined in this work. One may observe that the difference between them clearly tends to decrease from Gd^{2+} to Yb^{2+}.

To extract reliable values for $E(n, 2+, \text{A})$ from excitation and absorption spectra, knowledge of the energy level structure of the $4f^{n-1}5d$ configuration is required. Let us first ignore any interaction between the 5d electron and the electrons remaining in the 4f shell. The 5d electron interacts strongly with the crystalline environment, yielding a shift and a splitting of the degenerate levels into at most five distinct 5d states [13, 14]. They are denoted in order of increasing energy as $5d_1$ to $5d_5$. The $5d_1$ level combined with the lowest energy LS-term of the $n - 1$ electrons in the 4f shell are denoted as $4f^{n-1}[^{2S+1}L]5d_1$.

Experimental data show that the spin–orbit splitting of the lowest energy LS-term of $4f^{n-1}$ in the excited state configuration of the divalent lanthanide is practically the same as in the ground state configuration of the trivalent lanthanide ion. For example, the lowest levels of the excited configuration of Eu^{2+} are of the type $4f^6[^7F_J]5d_1$, where the ^7F term is spin–orbit split into the ^7F_J multiplets with $J = 0$–6. The energy difference between the multiplets are practically the same for the ^7F_J states of the ground state LS-term for the Eu^{3+} ion. This leads to the familiar 'staircase' pattern observed within the low energy part of the fd-excitation spectrum [18, 20]. Each step of the 6000 cm^{-1} long 'staircase' represents the next level of the ^7F_J multiplet. The 5d electron can also be found in higher 5d levels, and in most compounds the $4f^{n-1}[^7F_J]5d_2$ levels overlap with the first 'staircase', leading to broad excitation or absorption bands where all structure is washed out.

It is clear that in the case of Eu^{2+} one should not simply (as is frequently done) take the maximum of the broad excitation band to determine $E(7, 2+, \text{A})$. But instead one must determine the first step of the staircase located in the leading edge on the low energy side of the first excitation band. In principle, the same applies to the other divalent lanthanides. This difficulty does not arise for Yb^{2+} since the energy difference between the first $4f^{13}[^2F_{7/2}]5d_1$ and second $4f^{13}[^2F_{5/2}]5d_1$ 'step' is 10 300 cm^{-1} [22, 23]. Also for Tm^{2+}, Er^{2+} and Ho^{2+} the steps are well separated in energy [17, 24, 25]. The decoupled scheme works quite satisfactorily for the interpretation of the low energy part of the excitation spectra and it will be used throughout this work. In the next order of approximation one should include the exchange and Coulomb interaction between the $5d_1$ electron and the $4f^{n-1}$ electrons [21, 42]. The exchange interaction leads to the HS and LS states discussed above. They are denoted as $4f^{n-1}[^{2S+1}L_J]5d_1$ (HS) and $4f^{n-1}[^{2S+1}L_J]5d_1$ (LS). In practice, the spin-forbidden transitions to the HS states can only be observed for lanthanides with $n > 7$.

The Coulomb interaction creates additional fine structure in the $4f^{n-1}5d$ energy levels. We refer to the recent work by van Pieterson *et al* [26, 27]. Detailed experimental and theoretical information is provided on the $4f^{n-1}5d$ levels for the entire series of trivalent lanthanides in CaF_2, $LiYF_4$ and YPO_4. Results of that work are expected to apply equally well for the divalent lanthanides.

3. Presentation of the data

Prior to presenting how the data are obtained from spectra, results are already revealed in figures 3 and 4. $E(n, 2+, \text{A})$ of a divalent lanthanide is displayed against $E(7, 2+, \text{A})$ of Eu^{2+}. Data for Eu^{2+}, not shown in figures 3 and 4, then by definition fall on the drawn full lines of unit slope. If $E(n, 2+, \text{A}) - E(7, 2+, \text{A})$ does not depend on the type of compound, equation (3) applies and all data should fall on a set of parallel lines. For Sm^{2+}, Dy^{2+}, Tm^{2+} and Yb^{2+}, this appears clearly to be the case.

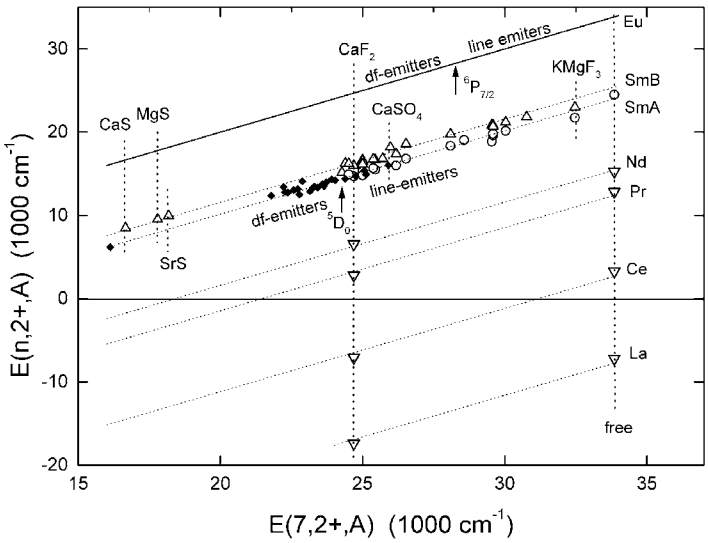

Figure 3. ▽, fd transition energies $E^{sa}(n, 2+, A)$ for La^{2+}, Ce^{2+}, Pr^{2+} and Nd^{2+} in compounds displayed against the transition energy for Eu^{2+}. △ and ○ are $E^{sa}(6, 2+, A)$ for the SmB and SmA band, respectively. ♦, $E_{em}(6, 2+, A)$ of Sm^{2+} displayed against the emission energy in Eu^{2+}. The broken lines are least square fits of lines of unit slope through the data. All data on Eu^{2+} fall on the full line.

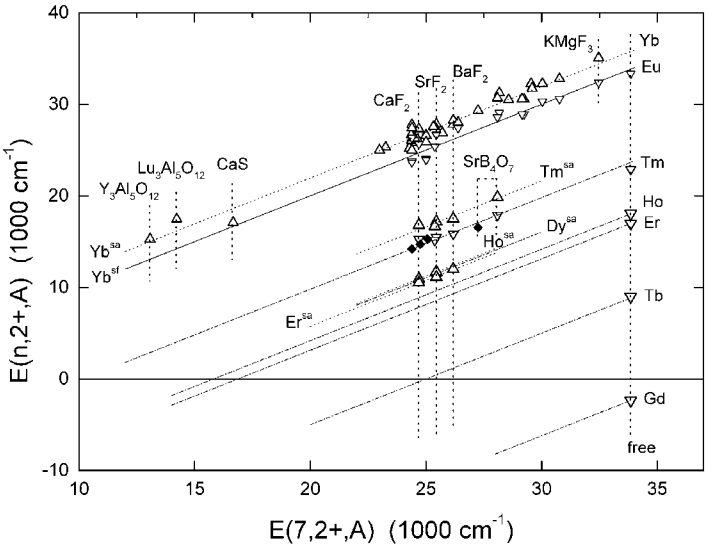

Figure 4. ▽, $E^{sf}(n, 2+, A)$ for Gd^{2+}, Tb^{2+}, Ho^{2+}, Er^{2+}, Tm^{2+} and Yb^{2+} displayed against the transition energy for Eu^{2+}. △, $E^{sa}(n, 2+, a)$ for Dy^{2+}, Ho^{2+}, Er^{2+}, Tm^{2+} and Yb^{2+} against $E(7, 2+, A)$. ♦, emission energy $E_{em}(n, 2+, A)$ for Tm^{2+} displayed against the emission energy in Eu^{2+}. The broken and chain lines are least squares fits of lines of unit slope through the data on spin-allowed and spin-forbidden transitions, respectively. Data on Eu^{2+} will fall on the full line.

Information on the 5d-level energies in La^{2+}, Ce^{2+}, Pr^{2+}, Nd^{2+}, Pm^{2+}, Gd^{2+}, Tb^{2+}, Dy^{2+}, Ho^{2+} and Er^{2+} is very scarce or even non-existent. The reason is that in compounds these lanthanides are very difficult to stabilize in the divalent state. Information that is available stems

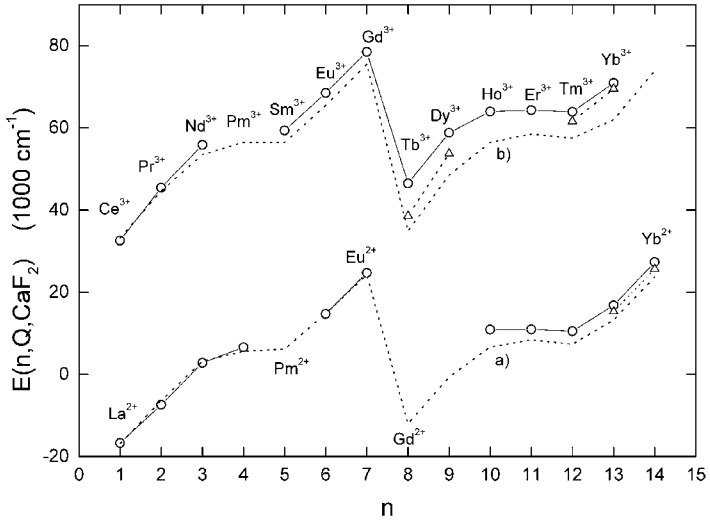

Figure 5. ○, experimental data on $E^{sa}(n, Q, \mathrm{CaF_2})$. △, data on $E^{sf}(n, Q, \mathrm{CaF_2})$. The data on $\mathrm{CaF_2}$:$\mathrm{Ln^{3+}}$ are from [11]. Curve (a): the free ion values $E(n, 0, 2+, \text{free})$ redshifted by 9650 $\mathrm{cm^{-1}}$. Curve (b): the free ion values $E(n, 0, 3+, \text{free})$ predicted by Brewer in [5] redshifted by 16 500 $\mathrm{cm^{-1}}$.

Table 1. The wavelength (nm) of the first spin-allowed fd transitions of the divalent lanthanides in $\mathrm{CaF_2}$, $\mathrm{SrF_2}$ and $\mathrm{BaF_2}$. For $\mathrm{Tm^{2+}}$ and $\mathrm{Yb^{2+}}$ the wavelength of a weak spin-forbidden transition is given within brackets. A negative value means that the 4f5d level is ground state.

$\mathrm{Ln^{2+}}$	$\mathrm{CaF_2}$	Reference	$\mathrm{SrF_2}$	Reference	$\mathrm{BaF_2}$	Reference
La	-600 ± 25	[16]				
Ce	-1350 ± 50	[38]		[39]		[39]
Pr	3570	[16]				
Nd	1520	[16, 40]				
Sm	680	[43, 62, 63]	645	[43, 63, 65]	625	[43]
Eu	405	[66, 67]	393	[66, 67]	382	[66, 67]
Dy	918	[16, 48, 68]	861	[72]	835	[72]
Ho	915	[16, 25, 47]	855	[25]		
Er	950	[16, 25]	900	[16, 25]		
Tm	595(655)	[17, 24, 46, 48]	582(646)	[17, 48, 69]	572(632)	[17, 48]
Yb	366(390)	[22, 80]	359(375)	[53, 80]	354	[80]

from studies mainly on $\mathrm{CaF_2}$, and occasionally on $\mathrm{SrF_2}$ and $\mathrm{BaF_2}$. Data for the lanthanides in these compounds are compiled in table 1.

The applicability of equation (3) is further demonstrated with the results on $\mathrm{CaF_2}$ shown in figure 5. Using for $E_{\mathrm{A\,free}}(n, 2+)$ the values of $E(n, 0, 2+, \text{free})$ in figure 2 together with $D(2+, \mathrm{A}) = 9650\ \mathrm{cm^{-1}}$, curve (a) is obtained. For $n \leqslant 7$, it shows a very good overlap with the experimental data. For $\mathrm{Tm^{2+}}$ and $\mathrm{Yb^{2+}}$, $E^{sf}(n, 2+, \mathrm{CaF_2})$ is about 2000 $\mathrm{cm^{-1}}$ larger than predicted from free ion data. Figure 5 also shows results for the trivalent lanthanides in $\mathrm{CaF_2}$. Redshifting the free ion values of curve (e) in figure 1 by $D(3+, \mathrm{CaF_2}) = 16\,500\ \mathrm{cm^{-1}}$ yields curve (b) in figure 5. By definition it coincides at $E(1, 3+, \mathrm{CaF_2})$ for $\mathrm{Ce^{3+}}$ but deviation from $E_{\mathrm{A\,free}}(n, 3+)$ increases with n until 6000 $\mathrm{cm^{-1}}$ for $\mathrm{Yb^{3+}}$. The values for $E_{\mathrm{A\,free}}(n, 3+)$ can be found in [11].

Below, for each individual lanthanide, data are commented on. Since the aim of this work is to demonstrate the validity of equation (3) for a wide range of different compounds, only data are presented where information pertaining to at least two different lanthanides in the same compound are available, see tables 2 and 3. We will start with Eu^{2+}. Because of its half-filled 4f shell, Eu^{2+} is the most stable divalent lanthanide, and it has been most widely studied. For that reason, Eu^{2+} serves as the reference divalent lanthanide in equation (3). It plays a similar role in this paper as Ce^{3+} for the trivalent lanthanides in [11].

$Eu^{2+}(n = 7)$

For the free ion, the transition to $4f^6[^7F_0]5d_1$ is observed at $E^{sa}(7, 2+, 0, \text{free}) = 33\,856\,\text{cm}^{-1}$. In compounds this first step of the 'staircase' can only be observed when the transitions to the $4f^6[^7F]5d_2$ states do not overlap with those to the $4f^6[^7F]5d_1$ states. This condition can be found in crystals providing large octahedral crystal field splitting of the 5d levels. Well resolved spectra are observed, for example, in $KMgF_3$ [28], EuF_2 [29], BaF_2 [30] and $Sr_3(PO_4)_2$ [31]. In those cases the first fd transition in Eu^{2+} can be determined with accuracy better than $\pm 500\,\text{cm}^{-1}$. However, the transition energy may also depend on temperature, Eu^{2+} concentration and method of crystal preparation, and in practice accuracy will not be better than $\pm 500\ \text{cm}^{-1}$. Frequently, a well resolved 'staircase' is not observed and a structureless $6000\ \text{cm}^{-1}$ or even wider broad band appears. In those cases, the wavelength where the excitation intensity has dropped to 15–20% on the long wavelength side of the first maximum will be regarded as a fair estimate for the location of the first 'step'. The typical error in the energy for the first fd transition can then be well above $500\ \text{cm}^{-1}$. Errors in $E(7, 2+, \text{A})$ for each compound individually are provided in [32]. Other errors may arise when the defect structure around Eu^{2+} is not precisely known. Particularly for the alkali-halides divalent lanthanides on the monovalent cation sites tend to aggregate. Such aggregates show different spectroscopic properties from isolated Eu^{2+}. These aspects have been very well studied, see for example [18, 33–35]. In the present work the data on isolated Eu^{2+} centres have been used.

After excitation of Eu^{2+} to the lowest 5d state, the surrounding lattice relaxes and df emission is Stokes shifted from the fd absorption. The emission wavelength is compiled in table 3. For the trivalent lanthanides it was found that the Stokes shift $\Delta S(3+, \text{A})$ is about the same for each lanthanide if at the same site in the same host crystal [11]. For the divalent lanthanides we expect similar behaviour, and for the df emission the following relation is anticipated:

$$E_{em}(n, 2+, \text{A}) = E_{\text{A free}}(n, 2+) - D(2+, \text{A}) - \Delta S(2+, \text{A}). \tag{4}$$

Figure 2 shows that for the free Eu^{2+} ion the $5d_1$ level is located above the $4f^7[^6P_{7/2}]$ level. Excitation to the $5d_1$ level is followed by relaxation to this $4f^7$ level, and narrow line $^6P_{7/2} \rightarrow {}^8S_{7/2}$ emission is observed. When $D(2+, \text{A}) + \Delta S(2+, \text{A})$ is larger than about $6000\ \text{cm}^{-1}$, the 5d level is shifted below the $^6P_{7/2}$ level and broad band df luminescence will take place. The location of the $^6P_{7/2}$ level more or less separating the 'line emitters' from the 'broad band emitters' has been indicated in figure 3. More information on the 'line emitters' can be found in [36, 37].

$La^{2+}(n = 1)$

$E(1, 0, 2+, \text{free}) = -7195\ \text{cm}^{-1}$, which means that in the free ion the 5d level is located below the $4f^1[^2F_{5/2}]$ level, see figure 2. In compounds one expects a dipole-allowed transition

Table 2. fd-absorption wavelengths (nm) of the divalent lanthanides in compounds. References to the literature for Eu data can be found in [32].

Compound	Eu	SmB	SmA	Sm reference	Yb^{sa}	Yb^{sf}	Yb reference
free	295		408	[2, 5]		300	[4]
$KMgF_3$ (K site)	308	435	458	[70, 71]	285	309	[52, 73]
$NaMgF_3$ (Na site)	325	460		[70]	305	327	[52]
$BaLiF_3$	333	472	496	[71, 74]	310	330	[75]
SrFCl	338	483	505	[76, 77]	315		[78]
BaFCl	338	480	510	[63, 72]			
$SrAlF_5$	339	480	530	[79]	310		[79]
$BaSO_4$	342				327	346	[54]
$SrSO_4$	343				327	346	[54]
BaB_8O_{13}	350		525	[81, 82]			
$LiCaAlF_6$	350				328		[73]
CaFCl	355				320	344	[78]
SrB_4O_7	356	506	545	[81, 83–85]	326	350	[86, 87]
$Sr_3(PO_4)_2$	367				341		[56, 88]
α-$BaCl_2$	377	538	595	[89]			
$CaSO_4$	379				357	365	[54]
BaF_2	382	575	625	[43]	354		[80]
KF	382				360		[23]
$REMgF_4$	385	550		[90]			
RbCl	389	595		[40, 92]	372		[91]
SrF_2	393	600	645	[43, 63, 65]	359	375	[53, 80]
$SrCl_2$	394	597	638	[64, 65]	363	394	[53, 93, 94]
CaB_2O (Si_2O_7)	395				363		[95]
KI	400	619	675	[92, 96, 97]	387		[23, 99, 100]
KBr	400	605	655	[92, 97, 98]	376	418	[23, 91, 99, 100]
KCl	400	600	665	[92, 97, 98]	376	416	[23, 91, 100, 101]
CaF_2	405	625	680	[43, 62, 63]	366	390	[22, 80]
$Ba_5(PO_4)_3Cl$: (6h)	406				382		[88]
$Sr_2B_5O_9Cl$: (site 1)	408	617	670	[85]	380		[103]
CaB(OH) (SiO_4)	410				365		[95]
NaBr	410				384		[23]
NaCl	410	615		[40, 92, 96, 97]	382	423	[23, 53, 102]
MgF_2	410				387	420	[52, 73]
Ca_2PO_4Cl: (site 1)	410				400		[88]
α-$Sr_2P_2O_7$	410				360	380	[56]
$Sr_2B_5O_9Br$: (site 1)	411				375		[103, 104]
NaI	412	660		[98]	398		[23]
$Sr_5(PO_4)_3Cl$: (6h)	430				395		[88]
Ca_2PO_4Cl: (site 2))	435				400		[88]
SrS	550	1005		[105, 106]			
MgS	562	1050		[57]			
CaS	600	1180		[106]	585		[107]
$Lu_3Al_5O_{12}$	703				573		[108]
$Y_3Al_5O_{12}$	765				655		[75, 108, 109]

to the $^2F_{5/2}$ and $^2F_{7/2}$ final $4f^1$ states separated by 1500 cm^{-1}. The only information available is on CaF_2 where the df transition is observed as a broad band (FWHM = 3000 cm^{-1}) around 556 nm [16]. This will be interpreted as the unresolved transition to the $^2F_{5/2}$ and $^2F_{7/2}$ levels. The transition to $^2F_{5/2}$ is then estimated at 600 ± 25 nm.

Table 3. df-emission wavelengths (nm) for the divalent lanthanides in compounds. When no references are given they can be found in table 2.

Compound	Eu	Sm	Yb^{sa}	Yb^{sf}	Tm^{sf}	Reference
SrB_4O_7	367			361	605	
$BaSO_4$	374			381		
$SrSO_4$	376			381		
$CaSO_4$	386	625		377		
α-$BaCl_2$	398	670				
I-$BaZnCl_4$	399	650			654	[51, 110]
$SrZnCl_4$	404	681			680	[51, 110]
$SrCl_2$	410	695	376	408	704	
SrF_2	416	703		800		
RbCl	417			426		[91]
$Sr_2B_5O_9Cl$: (site 1)	418	698		420		
$Sr_2B_5O_9Br$: (site 1)	422	715		421		[85, 103, 111]
KCl	423	740	395	432		
CaF_2	424	729		575		
NaCl	427	750	400	434		
NaBr	429	744				
KBr	430	750	399	443		[91]
KI	432	776	413	431		
$REMgF_4$	437	710				
NaI	439	800				
$CsRE_2I_5$	440	760				[112]
$RbRE_2I_5$	443	767				[112]
KRE_2I_5	447	785				[112]
$CsREI_3$	449	781		580		[112, 113]
$BaMgAl_{10}O_{17}$	450	746				[114–117]
$RbREI_3$	459	808		490		[112, 113]
SrS	620	1617				

$Ce^{2+}(n = 2)$

$E(2, 0, 2+, \text{free}) = 3277\ \text{cm}^{-1}$ and the lowest 5d level is located just above the $4f^2[^3H_4]$ ground state. In most compounds $D(2+, A)$ is larger than $3277\ \text{cm}^{-1}$, and the lowest fd state will be the ground state. This is the situation in CaF_2, see figure 5, where the df transition to $4f^2[^3H_4]$ occurs in the infrared at 1350 ± 50 nm [38]. Ce^{2+} was also studied in SrF_2 and BaF_2 [39], but unfortunately not in the infrared where the first df transitions are expected.

$Pr^{2+}(n = 3)$

With $E(3, 0, 2+, \text{free}) = 12\,847\ \text{cm}^{-1}$, Pr^{2+} is the first divalent lanthanide where in compounds the $4f^3$ configuration will usually provide the ground state. The only information found for compounds is for CaF_2 where the first fd transition is in the infrared, see table 1. df emission has not been reported. It is also not expected to occur since the 5d state will relax to one of the $4f^3[^4I_J]$ multiplets, see figure 2.

$Nd^{2+}(n = 4)$

Besides $E(4, 0, 2+, \text{free}) = 15\,300\ \text{cm}^{-1}$ only information on CaF_2:Nd^{2+} is available where the first fd transition is at 1520 nm [16, 40]. This places the 5d level amid the numerous $4f^4$ levels, and relaxation to them will prevent any df-emissive transitions.

$Pm^{2+}(n = 5)$

No information on df transitions is available for the radioactive Pm^{2+}. Based on ionization energies and other methods Brewer [2, 5] estimates a value of $16\,000 \pm 2000\ cm^{-1}$, Sugar and Reader [41] estimate $16\,400 \pm 2000\ cm^{-1}$ and Martin [3] estimates $17\,100 \pm 2500\ cm^{-1}$. Based on the present work and also on theoretical calculations by Sekiya *et al* [9], a value not much larger than that for Nd^{2+} seems likely. We will adopt $15\,800 \pm 1000\ cm^{-1}$ as the most likely value for $E(5, 0, 2+, \text{free})$.

$Sm^{2+}(n = 6)$

Sm^{2+} is relatively stable and spectroscopic information on Sm^{2+} in compounds is much more abundant than for La^{2+} to Pm^{2+}. Brewer predicts the lowest fd level ($^7K_4$) of the free ion at $E(6, 0, 2+, \text{free}) = 24\,500\ cm^{-1}$ [2, 5]. In the decoupled scheme, the low energy part of the fd-excitation spectrum of Sm^{2+} is related to the $4f^5[^6H_J]5d_1$ levels. The optical excitation spectrum of Sm^{2+} in CaF_2 was studied theoretically by Yanase [42]. It was shown that only transitions with $\Delta J = 3$ are allowed. This implies that, contrary to Eu^{2+}, not all transitions from the $J = 0$ ground state of Sm^{2+} to those of $4f^5[^6H_J]5d_1$ are allowed.

In the low energy part of the absorption/excitation spectra of Sm^{2+}, usually a main peak can be distinguished, sometimes accompanied by an unresolved and much (ten times) weaker shoulder band or tail on its low energy side. This is particularly clear in Sm^{2+} doped CaF_2, SrF_2 and BaF_2 where the main peak was designated as the SmB band and the satellite band as the SmA band [43]. Throughout this work we will use the same designation. The SmB band can often be determined with reasonable accuracy of about $400\ cm^{-1}$. The error in locating the SmA band can be quite large due to the weak intensity and unresolved nature of this band. Sometimes it could not be observed at all, and only information on the SmB band is then compiled in table 2.

Figure 3 shows that data on the SmA and SmB bands fall on lines parallel to that belonging to Eu^{2+} data. Even for the sulfides SrS and CaS, where the absorption is found in the infrared, the constant difference is maintained. This demonstrates that the redshift $D(2+, A)$ of the 4f5d levels in Sm^{2+} is the same as in Eu^{2+}. Extrapolating the data on the SmA band to the free ion situation yields $E_{A\,free}(6, 2+) = 24\,160\ cm^{-1}$, which is practically the same as the value for $E(6, 0, 2+, \text{free})$ predicted by Brewer. The SmA band should therefore be regarded as caused by the first fd transition. The weak intensity is attributed to the forbidden nature of the transition because of the $\Delta J = 3$ selection rule [21, 42]. The intense SmB band is now attributed to the first fd transition with $\Delta J = 3$. Averaged over 15 different compounds, the SmB band is found at $1410 \pm 360\ cm^{-1}$ higher energy than the SmA band.

Relaxation from the fd state down to the $4f^6[^5D_J]$ level will quench the df emission and narrow 4f → 4f line emission is observed instead, see figure 2. In the cases when the redshift $D(2+, A)$ and the Stokes shift $\Delta S(2+, A)$ place the fd level near or below the $^5D_0$ level, broad band df luminescence can be expected. Information on df emission is compiled in table 3 and displayed as $E_{em}(6, 2+, A)$ against the emission energy $E_{em}(7, 2+, A)$ of Eu^{2+} in figure 3. Data fall on the same straight line as those of the SmA band. This is a direct proof that the Stokes shift between absorption and emission in Eu^{2+} is the same as in Sm^{2+}, and it confirms equation (4). It also demonstrates that the SmA band must indeed be interpreted as the lowest $4f^5$5d level.

The location of the $^5D_0$ level is indicated in figure 3. It marks roughly the point separating the 'line emitters' from the 'broad band' emitters. The dividing point is, however, not sharply defined. The highest energy df emission was observed for $CaSO_4$:Sm^{2+} [44]. The emission

at 625 nm is at significantly higher energy than the line emission from the $^5D_0$ level observed around 685 nm. Apparently, the energy gap of 1400 cm^{-1} between the 5d and $^5D_0$ level makes the lifetime of the 5d state against multiphonon relaxation to the $^5D_0$ level just long enough to allow for the relatively fast df emission. Although relaxation to the $^5D_1$ level is very likely, emission expected around 630 nm was not observed. This need not be surprising because thermal excitation to the faster decaying 5d level will quench the $^5D_1$ emission.

$Gd^{2+}(n = 8)$

The HS $^9D_2$ fd level is the ground state in free Gd^{2+} with $E^{sf}(8, 0, 2+, \text{free}) = -2381$ cm^{-1} [45]. In compounds the energy of this level is decreased further. For Gd^{2+} in CaF_2 a wide absorption band between 500 and 600 nm is observed [46]. However, this cannot be the first df transition which is spin-forbidden and, according to figure 5, expected at 825 nm. Since no further information on compounds is available, the energy of the first LS $^7D_5$ fd level in the free Gd^{2+} at 6975 cm^{-1} will be adopted for $E^{sa}_{\text{A free}}(8, 2+)$.

$Tb^{2+}(n = 9)$

The first fd transition to the HS $^8G_{13/2}$ level is in the free ion at $E^{sf}(9, 0, 2+, \text{free}) = 8972$ cm^{-1}. For CaF_2:Tb^{2+}, a broad and structureless absorption band is observed between 450 and 650 nm [46]. With $D(2+, CaF_2) = 9650$ cm^{-1} the $^8G_{13/2}$ level will shift below the $4f^9[^6H_{15/2}]$ level. Since numerous low energy HS and LS fd levels exist overlapping strongly with the $4f^9$ levels, see figure 2, it is impossible to determine $E(9, 2+, A)$. The $^8H_{15/2}$ free ion level at 15 516 cm^{-1} is the first level that has a significant amount (19% of ^6H) of LS terms mixed in [4]. This level was adopted for $E^{sa}_{\text{A free}}(9, 2+)$ in figure 2.

$Dy^{2+}(n = 10)$

No information was found on the free Dy^{2+} $4f^9$5d levels. A value of 16 900 ± 1000 cm^{-1} for $E^{sf}(10, 0, 2+, \text{free})$ to the first HS state was estimated in [41]. Based on $E(10, 1, 1+, \text{free})$ and $E(10, 2, 0, \text{free})$, see figure 1, a value of 16 300 cm^{-1} will be adopted for $E(10, 0, 2+, \text{free})$ in this work. Data on transition energies to the first LS fd state are available on Dy^{2+} in the three alkaline earth fluorides, see table 1. They can be found in figure 4. Extrapolation in figure 4 to the free ion situation yields $E^{sa}_{\text{A free}}(10, 2+) = 20\,000$ cm^{-1} used for curve (b) in figure 2. Emission from the 5d states has not been reported.

$Ho^{2+}(n = 11)$

The first fd transition in the free ion is found at $E^{sf}(11, 0, 2+, \text{free}) = 18\,033$ cm^{-1} [5]. In compounds only data were found on CaF_2 and SrF_2 [16, 25, 47], see table 1. Like for Dy^{2+} the spectral bands should be attributed to the spin-allowed transitions. Extrapolation in figure 4 to the free ion situation yields $E^{sa}_{\text{A free}}(11, 2+) = 20\,240$ cm^{-1}. No df-related emission has been reported.

$Er^{2+}(n = 12)$

For Er^{2+} the exchange interaction between 5d electron and the 11 remaining 4f electrons is not very large, and a clear separation between LS and HS states is more difficult to make. The first fd transition in the free ion is found at $E^{sf}(12, 0, 2+, \text{free}) = 16\,976$ cm^{-1} which has mainly (at least 76%) HS character. At 18 976 cm^{-1} a level with 47% low spin ^3L character and at

20 226 cm^{-1} a level with 70% LS ^{3}I character is present [4]. In compounds only data were found on CaF_2 and SrF_2 [16, 25]. In absorption, four well separated broad (FWHM $\approx$ 1500 cm^{-1}) bands are observed, to be attributed to the spin-allowed transitions to $4f^{11}[^4I_J]5d_1$ (LS) final states with $J = 15/2, 13/2, 11/2, 9/2$ [16, 25]. Extrapolating the data in figure 4 to the free ion situation yields a value of 19 600 cm^{-1} for $E^{sa}_{\text{A free}}(12, 2+)$. It falls nicely between the first two states of the free ion containing a large fraction of low spin terms. No df-related emission was reported.

$Tm^{2+}(n = 13)$

The first level of the fd configuration is in the free ion at $E^{sf}(13, 0, 2+, \text{free}) = 22\,897$ cm^{-1}, and it has 81% HS ^{4}F character. The first level containing a large fraction (55%) of LS (^{2}K) terms is found at $E^{sa}(13, 0, 2+, \text{free}) = 25\,878$ cm^{-1} [4]. In CaF_2, the first strong absorption to a $4f^{12}[^3H_6]5d_1$ level is found at 595 nm. It should be attributed to the first spin-allowed transitions [17, 48]. At low temperature, a 15 times weaker satellite peak appears at 655 nm [24, 48]. It should be attributed to a spin-forbidden transition. Similar features were observed for SrF_2 and BaF_2, see table 1.

df luminescence was not reported for Tm^{2+} in the three fluorite crystals, but it has been observed [49–51] in SrB_4O_7, $SrCl_2$, $BaZnCl_4$ and $SrZnCl_4$, see table 3. Figure 4 shows that the data fall on the same line as the data for the spin-forbidden absorption. The conclusion is therefore that the reported emissions are all due to spin-forbidden df transitions. The 660 nm and the 30 times stronger excitation band at 600 nm in $SrCl_2$:Tm^{2+} should be attributed to the first spin-forbidden and spin-allowed transition, respectively [50].

Two more data points can be derived from the location of the zero phonon lines at 17 210 and 19 160 cm^{-1} for the first spin-forbidden and spin-allowed transition in SrB_4O_7:Tm^{2+} [49]. With a Stokes shift of 1360 cm^{-1}, 559 and 504 nm are anticipated for the maxima of the vibronic sideband positions of the first spin-forbidden and spin-allowed transitions. These data are also displayed in figure 4 and comply fully with expectation. Extrapolating the data in figure 4 to the free ion situation yields 25 500 cm^{-1} for $E^{sa}_{\text{A free}}(13, 2+)$ and 23 650 cm^{-1} for $E^{sf}_{\text{A free}}(13, 2+)$. They both agree well with the actual free ion values.

$Yb^{2+}(n = 14)$

As for Ce^{2+} the exchange interaction between the 5d electron and the single hole in the 4f shell is relatively weak, and the first levels of the $4f^{13}5d$ configuration contain both low spin and high spin LS-terms. A clear distinction between spin-forbidden and spin-allowed transitions cannot be made. The first level of the fd configuration in the free ion is at $E^{sf}(14, 0, 2+, \text{free}) = 33\,386$ cm^{-1} and the HS ^{3}P is the leading (97%) term. The next level is at 37 020 cm^{-1} with 54% of ^{3}H as the leading term [4].

The general appearance of the absorption/excitation spectra of Yb^{2+} in crystals providing sites of O_h point symmetry has been well described before [22, 23]. Strong and resolved spin-allowed excitation bands are observed for the alkali halides. The same applies to $KMgF_3$ and $NaMgF_3$ where, in addition, at 4 K a 20–40 times weaker excitation band is clearly revealed [52]. This band must be ascribed to the spin-forbidden transition. In many more compounds, a weak band or a faint tail reminiscent of the spin-forbidden transition can be observed that often was left unnoticed in the original papers. Data are compiled in table 2 and displayed in figure 4. Extrapolation to the free ion situation yields $E^{sf}_{\text{A free}}(14, 2+) = 33\,860 \pm 700$ cm^{-1} and $E^{sa}_{\text{A free}}(14, 2+) = 35\,790 \pm 700$ cm^{-1}. The first is, within error, the same as $E^{sf}(14, 0, 2+, \text{free})$. The second is 1230 cm^{-1} smaller than $E^{sa}(14, 0, 2+, \text{free})$.

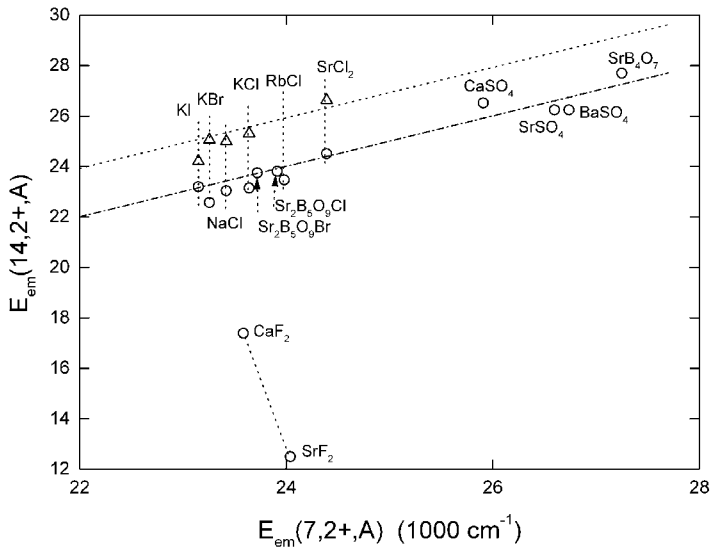

Figure 6. △, $E_{em}^{sa}(14, 2+, A)$ and ○, $E_{em}^{sf}(14, 2+, A)$ of Yb^{2+} in compounds displayed against $E_{em}(7, 2+, A)$ of Eu^{2+} in the same compound.

Data on the emission energy $E_{em}(14, 2+, A)$ are compiled in table 3 and displayed in figure 6 against the emission energy $E_{em}(7, 2+, A)$ in Eu^{2+}. The dotted and chain unit slope lines are the same as in figure 4, and one expects that the data should fall close to them. Information on a short decay time emission that can be identified as belonging to the spin-allowed Yb^{2+} df luminescence is limited to NaCl, $SrCl_2$, KCl, KBr and KI. Their data fall close to the dotted line in figure 6. Yb^{2+} in these compounds also show a slow emission that can be attributed to the spin-forbidden transition. Together with SrB_4O_7, the three sulfates and the two halo-borates data fall on the anticipated line. On the other hand, CaF_2 and SrF_2 show an anomalous behaviour in the sense that the emission is at much too long a wavelength.

4. Discussion

The data on Eu^{2+}, Sm^{2+}, Tm^{2+} and Yb^{2+} in figures 3 and 4 demonstrate that equation (3) holds for both the spin-allowed and spin-forbidden fd transition. The same applies (apart from CaF_2:Yb^{2+} and SrF_2:Yb^{2+}) for the data on df emission. The Stokes shift, being the difference between absorption and emission, should then be independent of the type of lanthanide ion. The Stokes shift $\Delta S(n, 2+, A)$, obtained from the data in tables 2 and 3, is displayed against the average Stokes shift in figure 7. Considering a typical error of 300 cm^{-1} in $\Delta S(n, 2+, A)$, the data available indeed display the same Stokes shift.

For the emission of Yb^{2+} in CaF_2 and SrF_2 the situation is, however, different. The Stokes shift is 8300 and 14 200 cm^{-1}, respectively, and data fall far outside the range of figure 7. This 'anomalous' behaviour has been studied by McClure and Pedrini [53] for Yb^{2+}-doped SrF_2. They showed that the 5d levels of Yb^{2+} are located inside the conduction band of the host crystal. Once excited, the Yb^{2+} will quickly auto-ionize and the 5d electron is transferred to conduction band states. The conduction band electron bonded to the hole on Yb forms an Yb-exciton-like state [53]. Electron–hole recombination may proceed radiationless or it

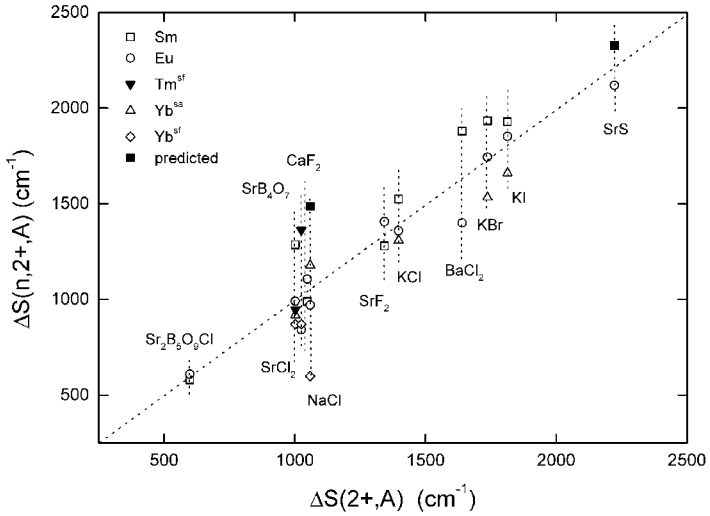

Figure 7. Stokes shift $\Delta S(n, 2+, A)$ of divalent lanthanides against the average Stokes shift $\Delta S(2+, A)$ in compounds.

may yield a strongly Stokes shifted emission. Such emission has been observed and studied in several other Yb^{2+}-doped compounds by Lizzo and co-workers [52, 54–56]. The fact that Eu^{2+} shows normal df emission in CaF_2 and SrF_2 suggests that for Eu^{2+} the lowest 5d band is located below the bottom of the conduction band. Since the anomalous emission is not due to df-transitions, it is not discussed further in this work.

With $E(7, 0, 2+, \text{free}) = 33\,856\ \text{cm}^{-1} \approx 34\,000\ \text{cm}^{-1}$, equations (3) and (4) can be used for predicting fd-absorption and df-emission energies once the redshift $D(2+, A)$ and Stokes shift $\Delta S(2+, A)$ are known for a specific compound. Using both emission and absorption data, the values for $\Delta E(n, 7, 2+)$ were calculated and compiled in table 4. The number N of data together with the standard deviation are given in table 4. In the cases where $N = 1$ there was no data available on lanthanides in compounds and the free ion values are compiled. For $N = 0$ even the information on the free ions is missing and the values estimated in section 3 are compiled. The information in table 4 was used to construct the set of parallel lines of unit slope through the data in figures 3 and 4. With $\Delta E(n, 7, 2+)$ inserted in equation (3) and with $D(2+, A) = 0\ \text{cm}^{-1}$, the values for $E_{A\,\text{free}}(n, 2+)$ used in figure 2 were obtained.

The standard deviation in $\Delta E(n, 7, 2+)$ for Sm^{2+}, Tm^{2+} and Yb^{2+} is of the same order of magnitude as the typical experimental error of $\pm 500\ \text{cm}^{-1}$ in the data of figures 3 and 4. Therefore, for these lanthanides there is no significant experimental deviation from equation (3). For La^{2+}, Ce^{2+}, Pr^{2+}, Nd^{2+}, Ho^{2+} and Er^{2+}, data is very scarce and one may question whether sufficient evidence is presented to use equation (3) for those lanthanides also. Three arguments can be given for further support.

(1) The data on CaF_2 shown in figure 5, at least for $n \leqslant 7$, vary in the same manner with n as the free ion data.
(2) Figure 1 shows that the systematics in the free lanthanides remains the same, irrespective of the ionic charge and the number of electrons in 6s.
(3) Equation (1) holds for the all the trivalent lanthanides in all compounds.

These arguments justify the main conclusion that equation (3) will hold for all 14 lanthanides in compounds like fluorides, chlorides, bromides, iodides, oxides and sulfides.

Table 4. $\Delta E^{sa}(n, 7, 2+)$ for spin-allowed and spin-forbidden transitions averaged over compounds A including free ion data. For Sm^{2+}, Tm^{2+} and Yb^{2+} both data from absorption and from emission were used. For Sm^{2+} data from the SmB band were also used. The total number of data N and the standard deviation is compiled. When $N = 1$, free ion data were used and when $N = 0$ anticipated values are given.

n Ln	$\Delta E^{sa}(n, 7, 2+)$	N	$\Delta E^{sf}(n, 7, 2+)$	N
1 La	$-41\,600 \pm 700$	2		
2 Ce	$-31\,170 \pm 850$	2		
3 Pr	$-21\,450 \pm 630$	2		
4 Nd	$-18\,400 \pm 320$	2		
5 Pm	$-18\,200$	0		
6 Sm	$-9\,840 \pm 360$	46		
7 Eu	0			
8 Gd	$-26\,900$	1	$-36\,200$	1
9 Tb	$-18\,500$	0	$-25\,000$	1
10 Dy	$-13\,940 \pm 220$	3	$-17\,700$	0
11 Ho	$-13\,760 \pm 10$	2	$-15\,820$	1
12 Er	$-14\,250 \pm 120$	2	$-16\,870$	1
13 Tm	$-8\,360 \pm 350$	5	$-10\,190 \pm 440$	10
14 Yb	$1\,930 \pm 670$	42	9 ± 700	29

In figure 1 it was demonstrated that the variation of $E(n, m, Q, \text{free})$ with n to a first approximation does not depend on m and Q. It was already established for the trivalent lanthanides that it also remains the same in compounds. In the present work the same conclusion can be made for the divalent lanthanides. The variation can be written as

$$\frac{\mathrm{d}E(n, Q, \mathrm{A})}{\mathrm{d}n} = \frac{\mathrm{d}I_{4\mathrm{f}}(n, Q, \mathrm{A})}{\mathrm{d}n} + \frac{\mathrm{d}E_{5\mathrm{d}_1}(n, Q, \mathrm{A})}{\mathrm{d}n}, \tag{5}$$

where $I_{4\mathrm{f}}(n, Q, \mathrm{A})$ is the energy required to remove an electron from the 4f shell and $E_{5\mathrm{d}_1}(n, Q, \mathrm{A})$ is the binding energy of the 5d electron in its lowest energy level. Two conclusions can be drawn.

(1) The ionization energy of the 4f electron provides by far the largest contribution to the overall variation of n, and $\mathrm{d}I_{4\mathrm{f}}(n, Q, \mathrm{A})/\mathrm{d}n$ is not much influenced by the host crystal. It is almost independent on the ionic charge, and for the free ions and atoms it is almost independent of whether the 6s shell is empty or filled with one or two electrons, see figure 1. Obviously the effective shielding of the 4f electrons by filled 5p and 5s shells is responsible for this behaviour.

(2) $\mathrm{d}E_{5\mathrm{d}_1}(n, Q, \mathrm{A})/\mathrm{d}n$ must be small and almost independent of the type of compound A. We also have to conclude that the interaction of the 5d electron with the crystalline environment is practically independent of the type of lanthanide ion. Possible variations with n should be systematic and independent of compound A.

Only under these conditions can equation (3) hold with a redshift $D(2+, \mathrm{A})$ that is the same for each lanthanide ion.

Equations (3) and (4) provide a powerful tool to predict fd-absorption and df-emission energies. One may simply shift the 5d levels in figure 2 downward by an amount $D(2+, \mathrm{A})$ to obtain the situation for each lanthanide in compound A. A further downward shift by $\Delta S(2+, \mathrm{A})$ provides the df-emission energy. Below, several applications of this predictive tool will be demonstrated.

(1) *Line emitters and broad band emitters.* The location of the lowest 5d level of the divalent lanthanides relative to the 4f levels can be read from figure 2 once $D(2+, \mathrm{A})$ is known.

Whenever the 5d level is isolated from lower lying 4f levels, one may expect to observe broad band df emission. Otherwise, due to multiphonon relaxation to the 4f levels narrow line ff emission takes place. In the case of the trivalent lanthanides, this same method was used by van der Kolk *et al* [1] to select compounds with ff line emission in Pr^{3+}.

(2) *Predicting the lowest 5d level in Sm^{2+}.* Often the weak ΔJ-forbidden transition, appearing as the SmA band in spectra, is not observed. However, since it always appears 1410 ± 360 cm^{-1} below the ΔJ-allowed transition its energy can be inferred from that of the SmB band. If the df emission is also known, an estimate for the Stokes shift can be made. Stokes shifts estimated this way for SrS and NaCl were also used in figure 7.

(3) *Identification of bands in spectra.* One may identify bands in spectra from information available on $D(2+, A)$. For example, in the optical stimulated luminescence (OSL) spectra of MgS:Ce^{3+};Sm^{3+} and MgS:Eu^{2+};Sm^{3+}, measured subsequent to exposure to ionizing radiation, a broad band peaking at 1050 nm was observed by Chakrabarti *et al* [57]. The authors propose for these materials a mechanism for the charge trapping and optically stimulated recombination. Electrons are trapped by Sm^{3+} to form Sm^{2+} and holes are trapped by either Ce^{3+} or Eu^{2+}. In the OSL process, the authors believe that the electron tunnels from an excited state of Sm^{2+} to Ce^{4+} or Eu^{3+}. The nature of the 1050 nm band was not further specified. Based on MgS:Eu^{2+} one obtains $D(2+, A) = 16\,200$ cm^{-1}. The location of the SmA and SmB band in MgS:Sm^{2+} is now anticipated around 1260 and 1070 nm, respectively. Clearly, the 1050 nm band in the OSL spectrum must now be interpreted as the allowed transition of the SmB band.

(4) *Prediction of (semi)-metallic properties.* Based on redshift values one may predict whether the lowest fd level will be the ground state. This may have quite drastic consequences for the properties of the compound when high concentrations of divalent lanthanides are present. The 4f state is a localized state without significant overlap between the 4f orbitals of neighboring lanthanide ions. On the other hand, the 5d orbitals are much more delocalized and significant orbital overlap exists. A conduction band may develop, leading to metallic or semi-metallic properties. This situation is expected to occur in all compounds with divalent La^{2+}, Ce^{2+} or Gd^{2+}. Indeed LaI_2, CeI_2 and GdI_2 are known to possess metallic properties [38, 58]. The same applies to PrI_2. NdI_2 shows an insulator to metal transition at high pressure [59]. Based on figures 3 and 4, it is predicted that CaS doped with large concentrations of divalent Pr, Nd, Tb, Er, Dy or Ho may reveal metallic-like behaviour. CeS is already known to show metallic-like conductivity and SmS behaves as a semiconductor [60]. The metallic properties of LaH_2 and the insulating properties of LaH_3, of current interest for the development of switchable mirrors [61], may also be directly related to the population of 5d states in the ground state configuration.

5. Summary and conclusions

Data has been obtained from a re-analysis of the literature on fd transitions in the divalent lanthanides in compounds. All data show that the characteristic variation in the fd-transition energy of the free ions and atoms in figure 1 remains practically the same for divalent lanthanides in compounds. Although some of these aspects were already known, the present work demonstrates that it holds for all the divalent lanthanides in a wide range of inorganic compounds (fluorides, chlorides, bromides, iodides, oxides, sulfides).

For the lanthanides with more than a half-filled 4f shell the transition to the first fd level is spin-forbidden. Often these spin-forbidden transitions were left unnoticed in the literature. In the present work these spin-forbidden transitions were identified both in absorption and in emission data. In the case of Sm^{2+} the first fd transition is ΔJ-forbidden. This transition

appears as a weak excitation or absorption band (SmA band) found in the low energy tail of the intense first ΔJ-allowed transition (SmB band).

The main objective of this work was to establish the validity of equation (3) for all the divalent lanthanides in a wide variety of inorganic compounds. It provides a powerful predictive tool since only the redshift $D(2+, A)$ for a compound is needed to obtain the fd-transition energy for each divalent lanthanide ion in that compound. Additional knowledge of the Stokes shift provides the df-emission energy for each lanthanide. In this work only data on compounds was presented where fd transitions are available for at least two different divalent lanthanides. There is, however, much more information. A study on Eu^{2+} providing values for $D(2+, A)$ and $\Delta S(2+, A)$ in about 300 different compounds will be presented elsewhere [32].

References

[1] van der Kolk E, Dorenbos P, Vink A P, Perego R C, van Eijk C W E and Lakshmanan A R 2001 *Phys. Rev.* B **64** 195129
[2] Brewer L 1971 *J. Opt. Soc. Am.* **61** 1666
[3] Martin W C 1971 *J. Opt. Soc. Am.* **61** 1682
[4] Martin W C, Zalubas R and Hagan L 1978 *Atomic Energy levels—The Rare-Earth Elements* NBS Circular (Washington, DC: US Government Printing Office)
[5] Brewer L 1983 *Systematics and the Properties of the Lanthanides* ed S P Sinha and D Reidel (Dordrecht: Reidel)
[6] Jörgensen C K 1962 *Mol. Phys.* **5** 271
[7] Nugent L J and van der Sluis K L 1971 *J. Opt. Soc. Am.* **61** 1112
[8] Nugent L J, Baybarz R D and Burnett J L 1971 *J. Inorg. Nucl. Chem.* **33** 2503
[9] Sekiya M, Narita K and Tatewaki H 2000 *Phys. Rev.* A **63** 012503
[10] Sugar J and Kaufman V 1972 *J. Opt. Soc. Am.* **62** 562
[11] Dorenbos P 2000 *J. Lumin.* **91** 91
[12] Dorenbos P 2000 *J. Lumin.* **91** 155
[13] Dorenbos P 2000 *Phys. Rev.* B **62** 15640
[14] Dorenbos P 2000 *Phys. Rev.* B **62** 15650
[15] Dorenbos P 2002 *Phys. Rev.* B **65** 235110
[16] McClure D S and Kiss Z 1963 *J. Chem. Phys.* **39** 3251
[17] Loh E 1968 *Phys. Rev.* **175** 533
[18] Rubio J O 1991 *J. Phys. Chem. Solids* **52** 101
[19] Meijerink A and Wegh R T 1999 *Mater. Sci. Forum* **315–317** 11
[20] Sugar J and Spector N 1974 *J. Opt. Soc. Am.* **64** 1484
[21] Payne S A, Chase L L, Krupke W F and Boatner L A 1988 *J. Chem. Phys.* **88** 6751
[22] Loh E 1969 *Phys. Rev.* **184** 348
[23] Bland S W and Smith M J A 1985 *J. Phys. C: Solid State Phys.* **18** 1525
[24] Kiss Z J 1962 *Phys. Rev.* **127** 718
[25] Kariss Ya E and Feofilov P P 1963 *Opt. Spectrosc. (USSR)* **15** 308
[26] van Pieterson L, Reid M F, Wegh R T, Soverna S and Meijerink A 2002 *Phys. Rev.* B **65** 045113
[27] van Pieterson L, Reid M F, Burdick G W and Meijerink A 2002 *Phys. Rev.* B **65** 045114
[28] Ellens A, Meijerink A and Blasse G 1994 *J. Lumin.* **59** 293
[29] Freiser M J, Methfessel S and Holtzberg F 1968 *J. Appl. Phys.* **39** 900
[30] Fuller R L and McClure D S 1987 *J. Lumin.* **38** 193
[31] Poort S H M, van Krevel J W H, Stomphorst R, Vink A P and Blasse G 1996 *J. Solid State Chem.* **122** 432
[32] Dorenbos P 2003 *J. Lumin.* submitted
[33] Hernandez J A, Cory W K and Rubio J O 1979 *Japan. J. Appl. Phys.* **18** 533
[34] Hernandez J A, Cory W K and Rubio J O 1980 *J. Chem. Phys.* **72** 198
[35] López F J, Murrieta H S, Hernández J A and Rubio J O 1980 *Phys. Rev.* B **22** 8428
[36] Blasse G 1973 *Phys. Status Solidi* b **55** K131
[37] Altshuler N S, Korableva S L and Stolov A L 1976 *Sov. Phys.–Solid State* **18** 679
[38] Alig R C and Kiss Z J 1969 *Phys. Rev.* **186** 276
[39] Pedrini C, Pagost P O, Madej C and McClure D S 1981 *J. Physique* **42** 323
[40] Johnson K E and Sandoe J N 1969 *J. Chem. Soc.* A 1694

[41] Sugar J and Reader J 1973 *J. Chem. Phys.* **59** 2083
[42] Yanase A 1977 *J. Phys. Soc. Japan* **42** 1680
[43] Wood D L and Kaiser W 1962 *Phys. Rev.* **12** 2079
[44] Calvert R L and Danby R J 1984 *Phys. Status Solidi* a **88** 597
[45] Callahan W R 1963 *J. Opt. Soc. Am.* **53** 695
[46] Merz J L and Pershan P S 1967 *Phys. Rev.* **162** 217
[47] Weakliem H A and Kiss Z J 1967 *Phys. Rev.* **157** 277
[48] Weakliem H A, Anderson C H and Sabisky E S 1970 *Phys. Rev.* B **2** 4354
[49] Schipper W J, Meijerink A and Blasse G 1994 *J. Lumin.* **62** 55
[50] Wenger O S, Wickleder C, Krämer K W and Güdel H U 2001 *J. Lumin.* **94/95** 101
[51] Wickleder C 2000 *J. Alloys Compounds* **300/301** 193
[52] Lizzo S, Meijerink A, Dirksen G J and Blasse G 1995 *J. Phys. Chem. Solids* **7** 959
[53] McClure D S and Pedrini C 1985 *Phys. Rev.* B **32** 8465
[54] Lizzo S, Meijerink A and Blasse G 1994 *J. Lumin.* **59** 185
[55] Lizzo S, Meijerink A, Dirksen G J and Blasse G 1995 *J. Lumin.* **63** 223
[56] Lizzo S, Klein Nagelvoort E P, Erens R, Meijerink A and Blasse G 1997 *J. Phys. Chem. Solids* **58** 963
[57] Chakrabarti K, Mathur V K, Rhodes J F and Abbundi R J 1988 *J. Appl. Phys.* **64** 1363
[58] Corbett J D, Sallach R A and Lokken D A 1967 *Adv. Chem. Ser.* **71** 56
[59] Meyer G 1991 *Eur. J. Solid. State Inorg. Chem.* **28** 473
[60] Samsonov G V 1965 *High Temperature Compounds of Rare Earth Metals and Non-metals* (New York: Consultants Bureau)
[61] Huiberts J N, Griessen R, Rector J H, Wijngaarden R J, Dekker J P, de Groot D G and Koeman N J 1996 *Nature* **380** 231
[62] Kaiser W, Garrett C G B and Wood D L 1961 *Phys. Rev.* **123** 766
[63] Mahbub'ul Alam A S M and Di Bartolo B 1967 *J. Chem. Phys.* **47** 3790
[64] Axe J D and Sorokin P P 1963 *Phys. Rev.* **130** 945
[65] Sorokin P P, Stevenson M J, Lankard J R and Pettit G D 1962 *Phys. Rev.* B **127** 503
[66] Moine M, Pedrini C and Courtois B 1991 *J. Lumin.* **50** 31
[67] Kobayasi T, Mroczkowski S, Owen J F and Brixner L H 1980 *J. Lumin.* **21** 247
[68] Kiss Z J 1965 *Phys. Rev.* **137** A1750
[69] Pedrini C, McClure D S and Anderson C H 1979 *J. Chem. Phys.* **70** 4959
[70] Valyashko E G, Bodrug S N, Krutikov A V, Mednikova V N and Smirnov V A 1978 *Opt. Spectrosc. (USSR)* **44** 425
[71] Gros A, Gaume F and Gacon J C 1981 *J. Solid State Chem.* **36** 324
[72] Kiss Z J and Weakliem H A 1965 *Phys. Rev. Lett.* **15** 457
[73] Kück S, Henke M and Rademaker K 2001 *Laser Phys.* **11** 116
[74] Meijerink A and Dirksen G J 1995 *J. Lumin.* **63** 189
[75] Henke M, Persson J and Kück S 2000 *J. Lumin.* **87–89** 1049
[76] Jaaniso R and Bill H 1991 *Phys. Rev.* B **44** 2389
[77] Schnieper M, Trotta F, Bersier S and Bill H 1999 *Appl. Phys. Lett.* **75** 40
[78] Schipper W J and Blasse G 1991 *J. Solid State Chem.* **94** 418
[79] Henderson E W and Meehan J P 1974 *J. Lumin.* **8** 415
[80] Moine B, Courtois B and Pedrini C 1989 *J. Physique* **50** 2105
[81] Qinghua Zeng, Zhiwu Pei, Qiang Su and Shihua Huang 1999 *Phys. Status Solidi* b **212** 207
[82] Qinghua Zeng, Zhiwu Pei, Shubing Wang, Qiang Su and Shauzhe Lu 1999 *Mater. Res. Bull.* **34** 1837
[83] Mikhail P, Hulliger J and Ramseyer K 1999 *Solid State Commun.* **112** 483
[84] Verwey J W M, Dirksen G J and Blasse G 1992 *J. Phys. Chem. Solids* **53** 367
[85] Dotsenko V, Radionov V N and Voloshinovskii A S 1998 *Mater. Chem. Phys.* **57** 134
[86] Blasse G, Dirksen G J and Meijerink A 1990 *Chem. Phys. Lett.* **167** 41
[87] Zhiwu Pei, Qiang Su and Jiyu Zhang 1993 *J. Alloys Compounds* **198** 51
[88] Palilla F C, O'Reilly B E and Abbruscato V J 1970 *J. Electrochem. Soc.: Solid State Sci.* **117** 87
[89] Lauer H V Jr and Fong F K 1976 *J. Chem. Phys.* **65** 3108
[90] Banks E, Nakajima S and Shone M 1980 *J. Electrochem. Soc.: Solid State Sci. Technol.* **127** 2234
[91] An C P, Dierolf V and Luty F 2000 *Phys. Rev.* B **61** 6565
[92] Bron W E and Heller W R 1964 *Phys. Rev.* **136** A1433
[93] Loh E 1973 *Phys. Rev.* B **7** 1846
[94] Piper T S, Brown J P and McClure D S 1967 *J. Chem. Phys.* **46** 1353
[95] Gaft M L and Gorobets B S 1979 *J. Appl. Spectrosc. (USSR)* **31** 1488

[96] Guzzi M and Baldini G 1973 *J. Lumin.* **6** 270
[97] Karapetyan V E, Maksakov B I and Feofilov P P 1963 *Opt. Spectrosc.* **14** 236
[98] Kaplyanskii A A and Feofilov P P 1964 *Opt. Spectrosc. USSR* **16** 144
[99] Wagner M and Bron W E 1965 *Phys. Rev.* **139** A223
[100] Pologrudov V V and Ibragim Z D 1999 *Phys. Solid State* **41** 1617
[101] Muller M, Fabris J L, Hernandes A C and Siu Li M 1993 *Phys. Status Solidi* b **180** K93
[102] Tsuboi T, Witzke H and McClure D S 1981 *J. Lumin.* **24/25** 305
[103] Dotsenko V P, Berezovskaya I V, Pyrogenko P V, Efrushina N P, Rodnyi P A and van Eijk C W E 2002 *J. Solid State Chem.* **166** 271
[104] Sidorenko A 2000 *Interfaculty Reactor Institute Report* No ST-ISO-2000-007 unpublished
[105] Robins L H and Ari Tuchman J 1998 *Phys. Rev.* B **57** 12094
[106] Gasiot J, Braunlich P and Fillard J P 1982 *Appl. Phys. Lett.* **40** 376
[107] Lehmann W 1972 *J. Lumin.* **5** 87
[108] Butaeva T I, Petrosyan A G and Petrosyan A K 1986 *Izv. Akad. Nauk* **24** 349
[109] Korzhik M V, Dobroshev G Yu, Kondratiev D M, Trower W P, Borisevich A E, Pavlenko V B and Timochenko T N 1996 *Phys. Status Solidi* b **197** 495
[110] Wickleder C 2001 *J. Lumin.* **94/95** 127
[111] Meijerink A and Blasse G 1989 *J. Lumin.* **43** 283
[112] Zhao Xinhua, Wang Shihua and Cao Baopeng 1992 *J. Alloys Compounds* **18** 235
[113] Xinhua Zhao, Yongzhi Deng, Zhonghe Li and Shihua Wang 1997 *J. Alloys Compounds* **250** 405
[114] Stevels A L N 1978 *J. Electrochem. Soc.: Solid State Sci. Technol.* **125** 588
[115] Verstegen J M P J and Stevels A L N 1974 *J. Lumin.* **9** 406
[116] Stevels A L N and Schrama-de Pauw A D M 1976 *J. Electrochem. Soc.: Solid State Sci. Technol.* **123** 691
[117] Ellens A, Zwaschka F, Kummer F, Meijerink A, Raukas M and Mishra K 2001 *J. Lumin.* **93** 147